CHAINSAW: Von-Neumann Accelerators To Leverage Fused Instruction Chains

Amirali Sharifian, Snehasish Kumar, Apala Guha, Arrvindh Shriraman
School of Computing Science
Simon Fraser University
{*amiralis, ska124, aguha, ashriram*}*@cs.sfu.ca*

***Abstract*—A central tenet behind accelerators is to partition a program execution into regions with different behavior (e.g., SIMD, Irregular, Compute-Intensive) and then use behavior-specialized architectures [1] for each region. It is unclear whether the gains in efficiency arise from recognizing that a simpler microarchitecture is sufficient for the acceleratable code region or the actual microarchitecture, or a combination of both. Many proposals [2], [3] seem to choose dataflow-based accelerators which encounters challenges with fabric utilization and static power when the available instruction parallelism is below the peak operation parallelism available [4].**

In this paper, we develop, *Chainsaw*, a Von-Neumann based accelerator and demonstrate that many of the fundamental overheads (e.g., fetch-decode) can be amortized by adopting the appropriate instruction abstraction. The key insight is the notion of chains, which are compiler fused sequences of instructions. chains adapt to different acceleration behaviors by varying the length of the chains and the types of instructions that are fused into a chain. Chains convey the producer-consumer locality between dependent instructions, which the *Chainsaw* architecture then captures by temporally scheduling such operations on the same execution unit and uses pipeline registers to forward the values between dependent operations. *Chainsaw* is a generic multi-lane architecture (4-stage pipeline per lane) and does not require any specialized compound function units; it can be reloaded enabling it to accelerate multiple program paths. We have developed a complete LLVM-based compiler prototype and simulation infrastructure and demonstrated that a 8-lane *Chainsaw* is within 73% of the performance of an ideal dataflow architecture, while reducing the energy consumption by 45% compared to a 4-way OOO processor.

1. Introduction

While it is clear that using customized hardware accelerators exploiting specific program behaviors is a promising way forward [1], it is not clear what is the particular accelerator microarchitecture and how can we achieve this efficiency while attaining the generality needed to support different applications. We have made great strides in cases where the hardware targets an already mature application domain (e.g., SIMD or GPUs). However, it is not clear how accelerators can be developed to address other programs that exhibit diverse control and memory behavior and instruction parallelism.

A central tenet of the modern accelerator proposals is to split up the program into multiple phases [10], and specialize the architecture for each behavior. Big and small cores [11], [12]) adopt this approach, but they tend to use a conventional front-end which dominates overall energy consumption [13]. Other approaches have sought to improve the general-purpose processor (herein referred to as *OOO*) efficiency by detecting and caching the loops in a smaller μop cache [14]. However, such approaches continue to rely on the energy-hungry backend of the processor such as a centralized register file and reorder buffer. Addressing these concerns, many hardware accelerator based approaches have eschewed the fetch-decode instruction model in favor of dataflow architectures [3], [15], [16]. SIMD-based designs amortize the cost of instructions across multiple data parallel operations but restrict the types of instructions that can be bundled and are closely allied to the hardware function unit. A key limitation of such dataflow approaches is designing for programs with varying levels of ILP. A reconfigurable functional-unit fabric [3] may have low utilization (and consequently higher static power) when the ILP in the programs do not match the peak ILP available from the hardware. It is hard to see how dataflow-based accelerators [6], [16], [17] can adapt to varied instruction parallelism both across applications and within an application. Section 3 discusses the tradeoffs in dataflow accelerators.

A promising approach to specialization is the notion of "custom or magic instructions" [7], [9], [13]. The key idea behind "magic" instructions is to use a single instruction to concisely express the parallelism and communication amongst frequently used groups of operations. Magic instructions require compound function units with associated lightweight storage elements that can execute these instructions efficiently. Magic instructions effectively amortize the cost of instruction fetch and decode across many operations. However, they tend to be application specific. Finding these magic instructions and then designing the custom function units that are widely used is challenging and raises questions about the generalizability of this approach. Nevertheless, the notion of using magic instructions to express more information about the program's operation flow to the hardware is a promising approach; except we focus on the question of *what property of the dataflow graph should magic instructions convey to the hardware* and *how do we decouple the hardware from the magic instruction itself* .

Our Contribution

In this paper, we explore *Chainsaw*, a von neumann-style accelerator, for executing *Chains*, which is a special type of magic instruction. The key contribution is that chains are decoupled from functional unit design, and are discovered at

978-1-5090-3508-3/16/$31.00

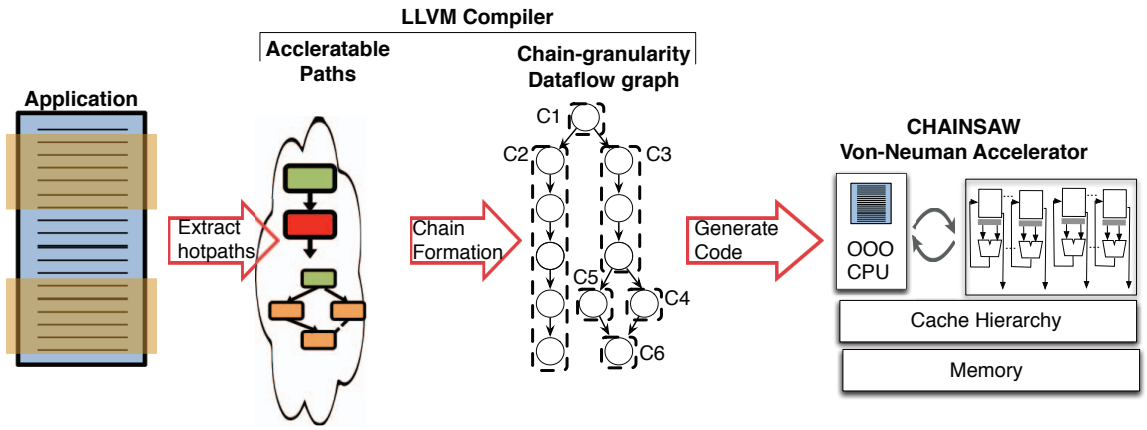

Figure 1: *Chainsaw* overview. Our compiler constructs control-free superblocks [5], [6] to eliminate branches from the offload region. The compiler then fuses sequences of instructions in the dataflow graph to construct chains (*C1, C2, C3* etc.) and statically schedules them on the *Chainsaw* multi-lane architecture at chain granularity. The unaccelerated program regions continue to run on the OOO. Compared to prior work that fused subgraphs [7]–[9] chains only fuse only sequences of operations and do not require specialized compound function units.

compile-time, thereby eliminating the tension between magic instruction efficiency and generality, application coverage and hardware design cost. A chain is a set of instructions that exhibits a strictly sequential dependence pattern i.e., each instruction in the chain strictly communicates only with the next instruction in the sequence. Chains are a generalization of the widely used fused multiply-and-accumulate instruction (a chain of an add and a multiply operation) or paired μops [18]. Converse to SIMD or VLIW instructions which express parallelism, chains express the lack thereof. Figure 1 shows our overall LLVM-based compiler and architecture framework and illustrates chains in the dataflow graph.

A chain concisely expresses producer-consumer locality between operations similar to dataflow. The limited single-producer to single-consumer locality expressed by chains can be i) more easily expressed with narrower instructions (i.e., no destination ops need to be specified) and ii) readily exploited using pipeline registers. We reduce back-end costs by temporally scheduling the entire chain on a single functional unit and then leverage pipeline registers to directly forward values between the instructions in the chain. This stands in direct contrast to energy hungry writes to a register file in an OOO and the operands transfers typically needed over a dataflow fabric [19] While chains can have a varied number of operations of various types, we restrict the number of live-ins and live-outs per chain to simplify the chain wakeup. Our accelerator, *Chainsaw*, exploits these chains to deliver highly efficient execution. Note that there are sections of the program where *Chainsaw* is not the most efficient execution engine (e.g,. SIMD, unpredictable control).

Chainsaw itself is a simple multi-lane architecture not too different from clustered [20]–[22] microarchitectures; each lane is a simple 4-stage in-order pipeline. While chains are mapped to individual lanes; the lanes execute at the granularity of the individual operations within a chain. Each lane executes only one chain at a time and does not interleave operations between chains which minimizes chain wakeup costs. The instruction parallelism is exploited across the lanes. Registers are only needed for inter-chain communication; bypass registers capture the intra-chain data movement. Similar to embedded processors [21], *Chainsaw* fixes the maximum number of instructions that can be mapped to a lane to minimize the fetch-and-decode costs. *Chainsaw* performs within 81% of an ideal CGRA accelerator. *Chainsaw* overhead to the processor core while saving 45% of the energy. Compared to a CGRA with 8$\times$ the resources Chains save between 24—54% of the communication power by localizing the communication and 21% of the static power by improving utilization of function units. We make the following contributions:

- We present a new instruction abstraction, Chains, that localizes communication between dependent instructions to minimize energy consumption. Chains do not require any custom function units.
- We develop a fully working prototype compiler based on LLVM to extract chains.
- We analyze chain formation algorithms for maximizing chain lengths (*MaxSize*) and ILP (*MaxILP*) and study the tradeoffs between increasing ILP and fusing operations to localize communication.
- We design the *Chainsaw* accelerator and evaluate its efficiency compared to a reconfigurable dataflow fabric (CGRA); we demonstrate the efficiency of *Chainsaw* for applications that do not possess high level of ILP.

The paper is organized as follows: Section 2 describes related ideas which inspire *Chainsaw*; Section 3 discusses the challenges with dataflow-based accelerators. Section 4 describes the tradeoff between different algorithms that the compiler prototype and tradeoffs when constructing chains. Section 5 describes the architecture and Section 7 presents the evaluation.

2. Related Work

Instruction set customization

The instruction abstraction plays a key role in permitting the compiler to express more information about the program control and dataflow structure to the hardware; for instance SIMD expresses data parallelism [20], [23], [24] between operations and VLIW expresses instruction level parallelism [20]. A pertinent question is what information about the dataflow structure do we expect instructions to express, can the information be expressed without increasing the size of the instruction, and does it generalize. Dataflow architectures [2], [3], [19] convey information about instruction dependencies and static placement of operations.

Tensilica [8], CCA [9], DSFU [7] have sought to extract commonly observed subgraphs of operations and then implement these operations using custom function units with associated storage elements. This effectively forms CISCy instructions and minimizes the energy overhead of the front-end. While this approach is promising for specific application domains it is not quite clear how it can be generalized especially given the need for specialized function unit. An interesting approach is the separation of compile-time ISA from the hardware ISA, an approach pioneered by Transmeta. Some have applied this idea [18] in a limited context for dynamically fusing pairs of x86 micro ops in a dynamic compiler to reduce the front-end overheads of an OOO.

Observations: Instruction-based specialization is an effective approach to reduce the overheads of the von neumann architecture. *Chainsaw* generalizes this approach and discovers new instructions from applications at compile time by aggressively fusing a variable number of operations and types of operations. An important challenge to be addressed is state management; as an increase in the number of operations expressed by an instruction makes it harder to manage the associated state. In this paper, we use the abstraction of chains which fuses only sequences of operations which minimizes the amount of state that needs to be maintained.

Efficient General-purpose Processors

Clustering of execution resources [20], [22], [25] seeks to scale up execution resources, localize communication between instructions, and minimize the cost of issuing instructions. These works minimized instruction-instruction communication by steering instructions to individual clusters of execution resources. In the past, these approaches have been pursued largely because of wire delays challenging pipeline design. Today, similarly with wire energy dominating overall instruction execution, clustering approaches can help improve energy efficiency. Another line of work [11], [12], [26] has used heterogeneous backends and schedule low-ILP or moderate ILP code regions on an inorder backend to save energy. A key limitation of past work is that they primarily focused on clustering backend resources while minimizing changes to frontend which expends a large fraction of the processor's energy. Loop-accelerators [14] recognized that the key to improving energy efficiency is to disable the front-end for repeating instructions; they also continue to use the backend of a general-purpose processor. Loop-accelerators do not localize communication between instructions and continue to use centralized register files, issue queues and execution units. Other work on increasing the front-end efficiency [27] has used out-of-order cores to generate schedules for in-order cores to execute. However, our focus is not just on in-order execution but also on minimizing back-end energy by localizing communication. There has been work in multi-level register files that have drawn ideas from embedded computing to exploit data locality at the fine-grain level between dependent instructions [21], [28]. A key benefit of this approach is that it generalizes how compound function units [6], [9], [15] achieve energy efficiency by using low energy operand registers to help dependent instructions directly communicate with each other.

Observations: When designing a von neumann based execution engine, we need to distribute the front and backend of execution to minimize the fixed overheads per instruction. *Chainsaw* uses a distributed lane-based execution model to localize communication between instructions and minimize the energy required to move data between dependent instructions. *Chainsaw* uses the compiler to identify and exploit the locality when moving values between dependent instructions. Compared to prior work that also sought to leverage fine-grain operand registers [21], *Chainsaw* develops a compiler framework to carefully fuse and organize the instructions to guarantee

Dataflow accelerators

Many recent proposals in hardware accelerators [2], [3], [29], [30] have been inspired by past work in dataflow architectures [19], [31]. These approaches have sought to switch between the von neumann execution on the general-purpose processor and the dataflow-based accelerator in a fine-grained manner [15]. Dataflow accelerators statically map at compile-time the program dependence graph to a fabric of homogeneous or heterogeneous function units to completely eliminate the overhead of fetch-and-decode. They also distribute the execution and register resources to improve scalability. However, dataflow accelerators tend to spatially distribute dependent operations and expend energy in moving data between the individual function units over the communication network. Dataflow accelerators are also by design more optimal when plenty of ILP is available in the program region; when there is only moderate levels of ILP they tend to idle the function units and have low utilization (and consequently higher static power).

Observation: A key challenge with dataflow accelerators is the energy required for moving values between dependent operations mapped across function units. *Chainsaw* temporally maps multiple dependent operations to the same function unit to minimize data movement. Dataflow architectures may seek to improve utilization by mapping multiple operations temporally to the same function unit; however, doing so would require a complex packet-based network [19]. Current accelerators use fine-grain instruction granularity PEs and implement circuit-switching; however such designs require a data transfer over the network for each producer-consumer dependency.

3. Background and Motivation

We motivate the chain abstraction for instructions using the DFG in Figure 2a. We are focusing on frequently executed regions that are free of control flow i.e. on hot paths or *traces* since these regions are the best candidates for acceleration. Therefore, the example dataflow graph (DFG) only depicts data dependencies. The DFG has a typical structure that is representative of hot paths in a wide variety of applications. It is an inverted tree that consumes several input values to output a few values at the bottom. The example DFG uses values computed by nodes (4), (13), (10), (7), and, (23), and produces values that are visible outside the DFG in nodes (26), and, (27). It has an ILP of five in the early three levels; in subsequent levels the ILP tapers off to two and then one.

Figure 2b and Figure 2c illustrate the differences between dataflow execution and von neumann execution applied to a subset of the DFG nodes. In the dataflow execution, functional units (FUs) are configured for specific operations, each node is statically mapped to a specific FU, and the dependencies are converted to data value transfers between the FUs. The von neumann execution shown here assumes just two FUs. These FUs are temporally reused by different nodes. To enable such temporal scheduling, instructions are stored in local instruction buffers and fetched, decoded and issued in order of dependence. The buffers may be local to FUs (as shown in the diagram) or global (fused). The results produced may be stored on the FU until it gets overwritten, or in local or global register files.

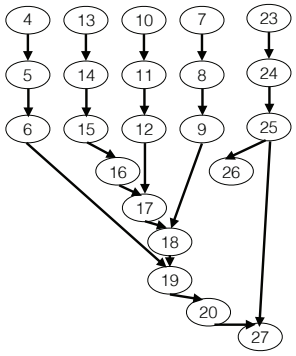

(a) Example DFG.

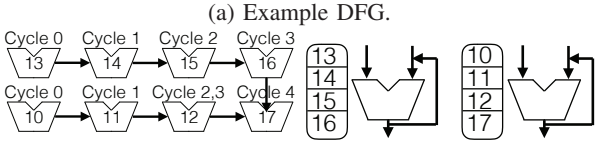

(b) Execution on a spatial fabric.

(c) Execution on a von neumann architecture.

Figure 2: Execution of DFG on spatial fabric leads to higher idleness in the spatial fabrics if the ILP in the application does not match the peak ILP of the spatial fabric and consequently static power will limit the overall power efficiency.

Fabric Utilization and Static Power: Executing the example DFG on a dataflow architecture with a single configuration pass will require at least as many FUs as there are nodes in the DFG. However, since the maximum ILP of this DFG at any level is five, at most five of the FUs can be active at any given cycle. All other FUs will be idle i.e. at least 17 FUs will be idle in any given cycle. Indeed, multiple instances of the DFG can be pipelined onto the dataflow architecture to reduce idleness, however the amount of reduction depends on the initiation interval. Unlike processor pipelines which are seeking to overlap pipeline stages, pipelining a dataflow graph requires the loop around the dataflow graph to be pipelineable i.e., overlapping multiple operations depends on the loop carried dependencies and unrolling factor. Even after pipelining iterations, the utilization of individual function units may be affected by the longest critical path in the DFG. For example, the FU allocated to node (12) must hold the result for an additional cycle (in cycle 3) while it waits for the result of (16) to materialize. Thus, this FU must incur one cycle of idleness as it is not on the critical path. Similarly, the function unit mapping (25) in Figure 2b has to wait for (20) to complete. Otherwise, a customized number of pipeline latches are needed between (25) and (27); clearly challenging [32].

TABLE 1: Characteristics of CGRA execution (4x4 and 8x8). Performance (cycles), Idle Cycles (cumulative function unit idle cycles). ILP: dataflow instruction parallelism

	#Ops in DFG	Avg ILP	CGRA 4X4		CGRA 8X8	
			Perf. Cycles	Idle Cyles	Perf. Cycles	Idle Cyles
gzip	59	5.1	117	1041	82	866
art	54	3.9	166	2076	128	1696
mcf	29	3.6	93	441	70	2612
equake	24	2.6	119	1106	96	3994
parser	38	4.7	102	1236	67	1958
bzip2	321	12.4	680	17856	437	35187
gcc	126	10.5	271	1782	183	1606
mcf	30	3.3	79	354	67	2474
namd	78	6	161	1158	137	7686
soplex	39	3.25	128	1522	122	3420
povray	95	6.78	191	1307	129	5373
hmmer	147	13.3	499	7792	287	14220
sjeng	99	5.8	219	4302	169	6356
h264ref	64	5.3	175	3420	157	10668
lbm	207	23	412	1847	242	13293
sphinx3	44	3.6	91	1350	88	4130
blacksc.	273	5.5	368	18257	275	25662
bodytra.	81	4.7	173	3780	118	6731
dwt53	33	3.6	102	1747	73	2480
fluidan.	70	4.1	184	2860	132	8676

Table 1 shows the idle cycle count for spatial fabrics of size 4x4 and 8x8. In this table, idleness is defined as the total number of cycles for which the function units are idle. In this case, we are modeling an instruction granularity CGRA with one function unit per PE, and we assume an ideal memory system to eliminate the stalls due to the memory system. The idle cycles in the table are hence indicative of the idleness caused entirely by the mismatch between the ILP available in the program and the ILP of the CGRA; making the CGRA smaller would increase the reconfiguration frequency and overhead. The idleness in the 8x8 (64 units) fabric is average 2$\times$ compared to the 4x4 (16 units) fabric (max: povray. 4$\times$ the idleness). Idleness is a critical factor because it determines the static power consumption of the fabric and as can be seen, the cumulative idle cycles are many times the execution

latency. In some cases, the 4× can have idleness higher than the 8*x*8; this may seem counter-intuitive; we discuss below.

Reconfiguration costs: Idleness could be reduced by reducing the number of FUs available, however in that case, the dataflow architecture must be reconfigured multiple times to execute a single instance of the DFG, and the pipelining opportunities are also limited. Since reconfiguration costs are significant, this is not always a viable solution.

Table 1 shows the average number of operations in the dataflow fabric. The fabric may need multiple passes to map the dataflow graph since the number of operations exceeds the number of function units in the fabric. However, the ILP column indicates that the dataflow graph will typically not be able to keep all the function units busy leading to uneasy tradeoff between static power and reconfiguration overheads. We illustrate the counter intuitive case introduced by the reconfiguration in gzip; in gzip the 4*x*4 demonstrates more idleness than the 8*x*8. Multiple reconfigurations introduce an unbalanced execution in the 4*x*4; gzip has 59 ops requiring 3 reconfigurations on a 4*x*4 (16 units) fabric with the final configuration leaving 5 PEs free for the entire duration of running the final 11 operations on a small fabric. All 59 ops can be mapped to 8*x*8 at once leading to lower idle cycles.

Data Movement Energy:

Dataflow accelerators at the instruction granularity maintain a 1:1 mapping between operations and function unit [32] to enable the use of a circuit switched network for the dataflow transfers. While this minimizes the per-transfer overhead, every producer-consumer operation communication requires a network transfer. Under current technology constraints we show that this can consume a significant fraction of the overall power consumption [33].

Interestingly, while Von-Neumann architectures temporally map multiple operations to the same function unit. This captures the locality between back-to-back dependent operations by forwarding values through pipeline registers. For example, just five FUs can capture the maximum ILP presented by the example DFG, minimizing idle cycles. The efficiency of von neumann architectures depends heavily on instruction granularity [18]. Coarse-grain instructions can potentially reduce front-end overhead and exploit locality between operations [13] However, they may adversely affect scheduling complexity due to dependency checks i.e. they consume and produce more values. To make coarse-grain instructions feasible we need to group operations without increasing the number of external dependencies. Hot regions in programs typically exhibit instruction sequences that meet these requirements. The example DFG is composed of several chains of computation that have the properties we are looking for: $(4,5,6)$, $(13,14,15,16)$, $(10,11,12)$, $(7,8,9)$, $(23,24,26)$, and, $(19,20)$. The *Chainsaw* accelerator leverages such chains for greater efficiency.

4. Our proposal: Chains

In this section, we propose *Chains* as a new instruction abstraction for representing computation to the hardware. Chains are fused sequences of operations where at least one of the instruction's operands is produced by the previous instruction. Also, the outputs of chains become visible to other instructions only when the chain in entirety is completed regardless of when the values are actually produced, to minimize dependence tracking and chain wakeup costs.

Listing 1: Algorithm for the *MaxSize* strategy.

```
for each edge {
    src_node = source(edge);
    tgt_node = target(edge);
    src_chain = chain(src_node);
    tgt_chain = chain(tgt_node);
    if (src_chain == tgt_chain)
        continue;
    tmp_chain =
        concat(src_chain, tgt_chain);
    if (live_ins(tmp_chain) > 2)
        continue;
    if (live_outs(tmp_chain) > 2)
        continue;
    remove src_chain from dfg;
    remove tgt_chain from dfg;
    add tmp_chain to dfg;
    if (dfg has cycle) {
        remove tmp_chain from dfg;
        destroy tmp_chain;
        add src_chain to dfg;
        add tgt_chain to dfg;
    } else {
        destroy src_chain;
        destroy tgt_chain;
    }
}
```

Figure 3a shows a possible decomposition of the dataflow graph in Figure 2a into chains; there are five chains, *C*0—*C*4. This decomposition has been produced using the Dilworth chain decomposition algorithm [34]. Note that the original Dilworth decomposition may produce dependency cycles among chains, which are not allowable in our case since such chains cannot be temporally scheduled. Therefore, we applied Dilworth decomposition and then broke the cycles by breaking the chains at cycle-forming dependencies.

Figure 3a also depicts a possible chain schedule if two FUs are available. Each chain node has a height that is directly proportional to its latency. Chains *C*4, *C*3 and *C*1 are scheduled on one functional unit in that order, while *C*0 and *C*2 are scheduled on the other unit in that order. Note that (25) in chain *C*4 supplies a value to chain *C*1. This value is produced before *C*4 completes execution; however since *C*4 can only communicate the value at the chain boundary, *C*1 is stalled until all the instructions in *C*4 complete.

Chains are essentially a ISA abstraction between the compiler and the hardware i.e., they do not need any specialized function units. The computation within the chain is expressed as stripped out instructions of the original processor ISA. The communication to the operations within a chain are restricted. One of the operands for each internal instruction will be the produced by the predecessor instruction in the chain. Leveraging this observation we eliminate the bits reserved in an instruction for register ids, compresses the instruction and reduce the fetch-decode penalty.

Chains provide the following benefits: 1) they localize a large fraction of communication between dependent instructions and eliminate many register accesses 2) they reduce the number of front-end events and exploit the ILP effectively. For instance, while the dataflow graph had 21 dependencies communicated through registers before chaining, chaining reduces the number of register writes to 4. Finally, due to the adoption of the von neumann model, we need fewer FUs than a spatial fabric by temporally mapping multiple operations to the same function unit, resulting in better hardware utilization and larger dataflow graph mapping. In this section, we explore questions that are critical to the success of chains: 1) Are chains potentially beneficial? and, 2) Is chain management hardware-friendly?

4.1. Are chains potentially beneficial?

Before we explore the potential benefits of chaining, we discuss the potential drawbacks and our strategies for minimizing these drawbacks. Chaining potentially decreases available ILP because instructions may need to wait for their chain to be activated even though their input operands are already available. The chain is activated only when the input operands are available for all the constituent instructions. This impact is visible in Figure 3a. Although instruction (13) is ready to run at the very outset, it cannot execute until the chains *C*0, *C*2, *C*3, and, *C*4 have finished.

Therefore, to recover lost ILP, we break chains at inter-chain dependencies as shown in Figure 3b. Thus, for example, instructions (16) and (17) have been assigned to different chains. Now, chain *C*1 can be scheduled at the beginning since it does not depend on any other chain. Indeed, the latency of the region decreases from 16 cycles to 13 cycles, as shown in Figure 3b. We also ensure that both the live-in count and the live-out count of each chain are limited to two, for reasons that are discussed in Section 4.2. Breaking at every live-in limits the number of chain inputs to two because now a chain has at most one node that consumes live-ins, and operations need at most two operands. However, the value produced by a node may be consumed by more than two nodes. In such a case, we introduce dummy fan-out nodes to limit the fan-out of each node to two. Essentially,

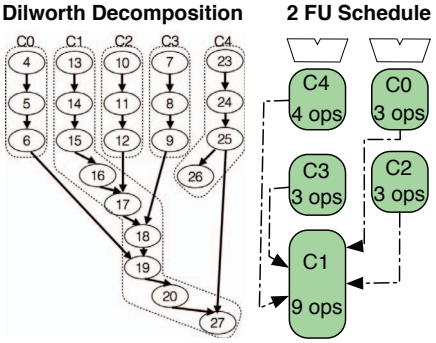

(a) Chains built using Dilworth decomposition followed by cycle removal. Chain schedule on two FUs; the height of a chain is proportional to the number of ops in it. Fusing operations to chains reduce inter-chain register writes (21 to 4). Chains can exploit ILP with only two FUs (latency: 16 cycles for DFG).

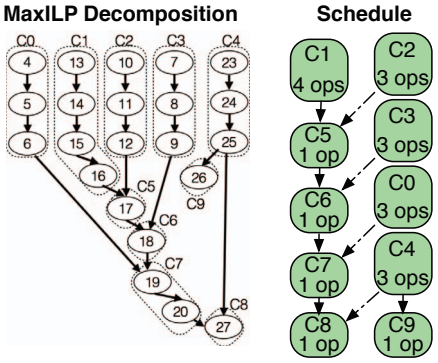

(b) Strategy *MaxILP* breaks chains at live-ins and live-outs leading to shorter chains and a higher chain count. More inter-chain data movement but critical path reduces to 13 ops, identical to the unchained DFG. Inter-chain register writes increased to 9.

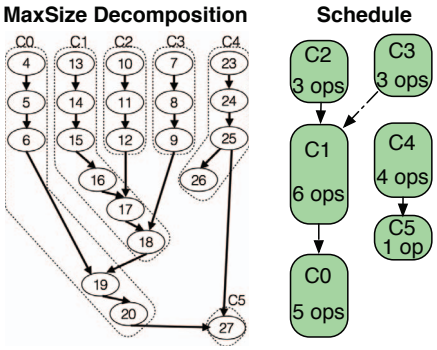

(c) Strategy *MaxSize* merges chains greedily to reduce data movement. Register writes decreased to 4. Critical path length increased to 14 ops.

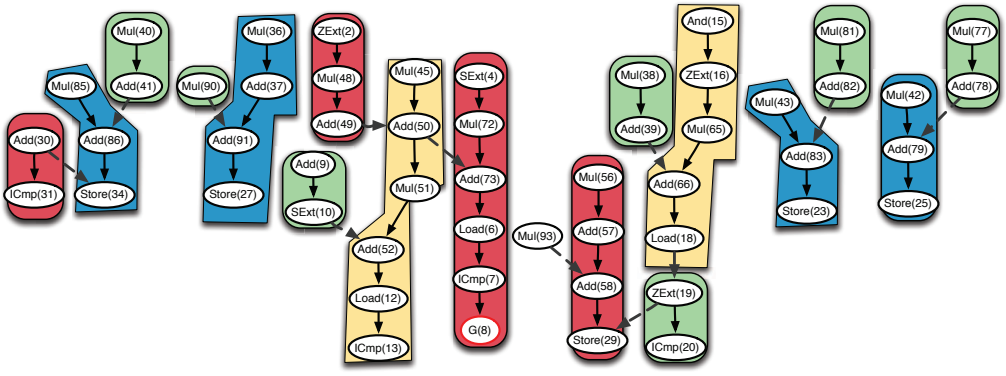

(d) The chained graph for a frequently executed region in *gzip*. The DFG has varying levels of ILP which is unsuitable for spatial fabrics, and has several long chains.

Figure 3: Chain Formation

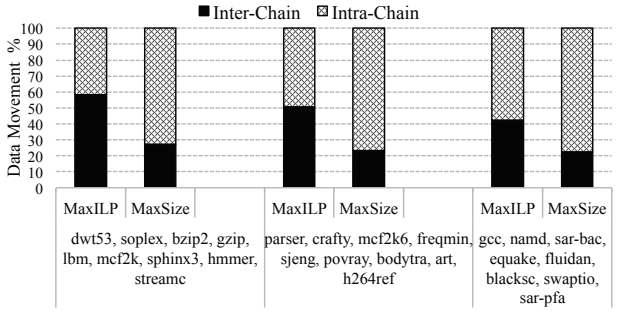

(a) Relative proportion of inter-chain and intra-chain dependencies. Fusing ops into chains localizes communication.

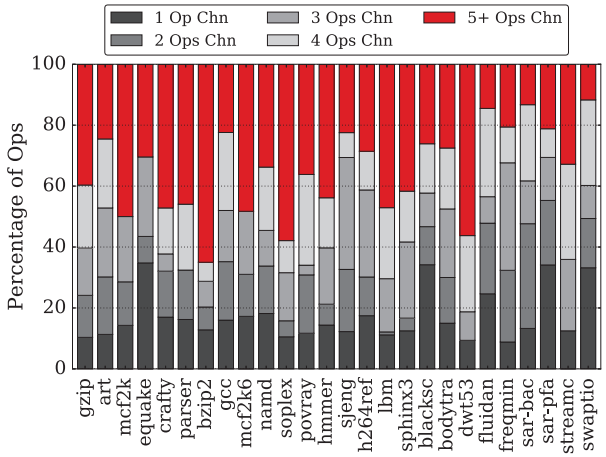

(b) Computation coverage by chains. Histogram showing the percentage of ops subsumed by chains of different lengths. 50–80% of operations are subsumed by chains of length 3 or more.

Figure 4: Potential for computation localization by chains.

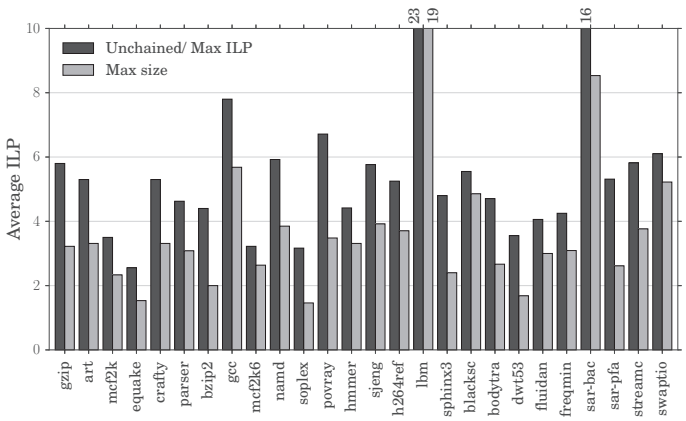

Critical Path Increase (MaxSize vs Ideal Dataflow)	
<20%	blacksc., swaptio, lbm, mcf, hmmer, fluidan.
20—40%	freqm., h264re., sjeng, parser, mcf, namd, streamc, art, crafty
50%	equake, bodytrack, gzip, sar-backprojection, povray, sphinx3, sar-pfa-interp1, dwt53, soplex, bzip2

Figure 5: The amount of ILP mined from the dataflow graph by the MaxILP and the MaxSize algorithms. MaxILP has average ILP that is equal to the unchained dataflow graph's ILP. MaxSize shows notable ILP loss in some applications.

each fan-out dummy node acts as a switch with a fan-in of one, and a fan-out of two. We denote this strategy as *MaxILP*.

Splitting chains reduces some of the benefits because intra-chain dependencies are converted into inter-chain dependencies which need register updates. For example, the MaxILP strategy produces 9 inter-chain dependencies while the baseline decomposition required 4. To offset the loss, we merge back chains greedily as long as they do not form cycles. We continue to limit both the live-in and live-out counts of each chain to two. Listing 1 lists the pseudocode for this strategy. It iterates over each edge, and if the edge happens to be an inter-chain dependency, the algorithm explores concatenating the source and sink chains. We denote this chain formation strategy as *MaxSize*. For example, the chain decomposition in Figure 3b is converted to the chain decomposition in Figure 3c. The overall latency increases to 14 cycles, but the number of external dependencies reduces to four.

Figure 3d shows the chained graph for a frequently executed region in *gzip*. The colors red, blue, green, and, yellow depict the nodes and edges belonging to a particular chain. Some binary operations such as multiply are shown to have zero or one inputs because either the inputs are data values produced outside the region, or are constants. The dataflow graph shows varying amounts of ILP at different levels which is unsuitable for spatial fabrics. At the same time, the dataflow graph exhibits long chains that can be exploited by *Chainsaw*.

There is a tension between chain size and average ILP. Chains are beneficial if the ratio of intra-chain dependencies to inter-chain dependencies is high and the impact on ILP is minimal. Figure 4a shows the relative proportion of internal and external dependencies using the MaxILP and MaxSize strategies respectively. For the MaxSize strategy, 70-80% of the dependencies have been converted to intra-chain operations, which will lead to high efficiency benefits in chained execution. The conversion rate is significantly lower at 40-60% for the MaxILP strategy. Figure 4b elucidates the reason for the high rate of conversion by the MaxSize strategy. Each stacked bar shows the relative proportion of dataflow graph nodes in chains of different lengths i.e. the percentage of computation covered by chains of different lengths. For MaxSize strategy, 50-80% of the nodes belong to chains of length three or more i.e. most nodes belong to reasonably long chains. *bzip2, soplex, lbm* and *dwt53* have 50% of the chains with more than 5+ ops. *equake, blackscholes*, and *swaptions* have dataflow graphs that are closely interleaved leading to small chains; $\simeq$35% of the operations have only one op. Figure 5 shows the average ILP in dataflow graphs for both the strategies as compared to the ILP in the unchained state. Since the MaxILP algorithm forcefully breaks the chain when any internal instruction

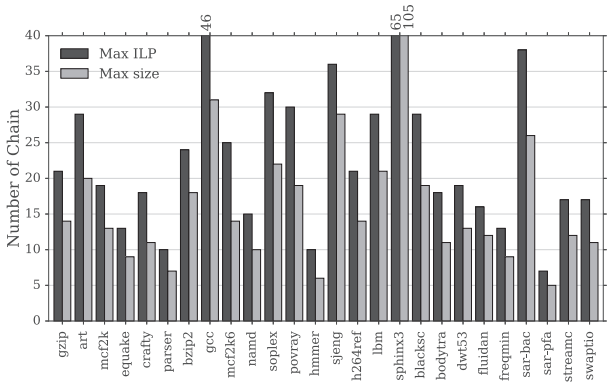

(a) # of chains generated by the MaxILP algorithm and the MaxSize algorithms. MaxSize typically creates fewer chains enabling.

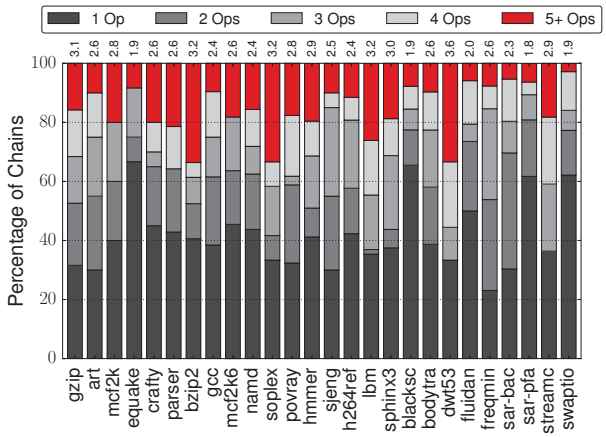

(b) Average chain lengths generated by MaxSize algorithm.

Figure 6: Properties showing the feasibility of implementing a chain–based architecture.

has an external dependency it attains as much ILP as the original unchained dataflow graph. The MaxSize algorithm may potentially lose ILP, when an internal operation in the chain is delayed from waking up a remote chain. The loss in ILP may also manifest as an increase in the critical path when compared to the ideal unchained dataflow graph. Our model here assumes every instruction in the critical path has the same latency to eliminate effects of memory operations. Overall, we find that in 6 applications chains increase the critical path by $<$20% and lose avg. 20% of the ILP. In 5 applications (sphinx3, sar-pfa, dwt53, soplex, bzip2) we reduced the ILP by 2$\times$ compared to the ideal dataflow graph. Note that these are averages and in many cases as long as we don't restrict the ILP at particular points of the dataflow graph (e.g., memory ops) the overall performance won't necessarily suffer. In summary, chains have a high potential for improving energy-efficiency.

4.2. Chain Distribution

Figure 6b shows the distribution of chains by size per application. The average chain size per application is presented at the top of the chart. Overall, the average chain length is 2.6 operations across benchmarks Apart from 4 applications (183.equake, blackscholes, sar-pfa and swaptions), all other applications have 50% or more chains with size greater than 2. Figure 6a shows the number of chains per application. The MaxILP approach produces significantly more chains than the MaxSize approach as described previously in § 4. There are 30 chains per workload on average, 10 workloads have fewer than 20 chains. Only 482.sphinx3 has more than 60 chains (avg. size 3). In conclusion, the number of chains per workloads is a tractable for frequently executed regions.

5. Architecture

Figure 7 describes the overall *Chainsaw* design. *Chainsaw* is a multi–lane design consisting of *lanes*, each of which contains a 4–stage single–issue pipeline which fetches and decodes instructions from an instruction buffer. Each chain is scheduled in entirety on a single lane to exploit the intra-chain locality within the lane's pipeline registers. The instruction buffer stores the execution sequence for multiple chains and chains are executed out-of-order as they are activated. Chains communicate with each other through registers; the live-in register bank holds the values for the duration of a chain's execution. Chains only write out the live–out values into the register once they complete all the operations in the sequence. Each lane has a pair of input registers, $IN0$, and, $IN1$ to hold the live-in values for the duration of an executing chain; these are refilled from the live-in register file when a chain is scheduled on the lane. If a chain produces values that will be consumed outside itself, these values are placed in a pair of output registers, $OUT0$, and, $OUT1$. The INs and the OUTs essentially act as a local register file (refilled and written back at chain boundaries).

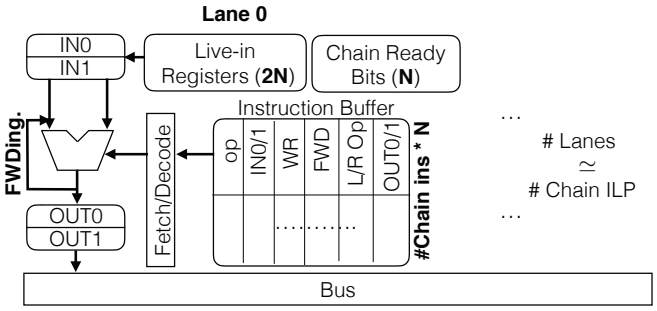

Figure 7: Block diagram of the Chainsaw accelerator. It is composed of lanes. Each lane has a INT and FPU with forwarding registers, two input/output registers (INs and OUTs), a live-in register bank, and an instruction buffer. Instruction fields: op=opcode, IN0/1: Operand consumes IN0 or IN1 live in value, WR: does instruction produce live-out?, FWD: Foward value to subsequent instruction, L/R Op: operand order (is the IN the left or right operand of the instruction), the other operand is the forwarded value. OUT0/1=write output to register OUT0 or OUT1.

They help indirectly minimize the fetch-decode energy by restricting the number of bits required to encode the register names i.e., instructions within a chain can only refer to 2 INs

or 2 *OUT*s (2 bits for encoding) as opposed to register names (8 bits or more). When a chain finishes, a bus routes values in the output registers to the appropriate bank if required. Finally, a scheduler determines when to schedule each chain in the DFG. Each lane includes a `Chain Read` bitmap which specifies the chains ready for execution. The number of entries in this table specifies the maximum number of chains that can be mapped to that lane; each entry is 10 bits wide; two 4–bit fields specifying the live-in register ids in the bank and two flag bits for registering the completion of the parent chains. All other structures also need to be proportionately scaled based on the `Chain Ready` bitmap (*N*), where *N* is the number of chains; the number of live-in registers is (2×N) which the compiler guarantees when forming the chains. The number of entries in the instruction buffer determine the maximum size of each chain; here we set it to the average sizeof(Chain)×N. The number of lanes is proportional to the ILP available.

Execution

The instruction buffers in each lane are preloaded before *Chainsaw* starts execution; the reconfiguration involves writing the instructions into the instruction buffer. Chains are statically mapped onto lanes to ensure that the requirements for the instruction buffer and the live-in register bank does not exceed availability. However, chain activation is carried out dynamically to improve latency. When a lane becomes available, the scheduler checks for chains that are ready i.e. chains that have been mapped to the available lane by the compiler and whose live-in values are all available. It activates one of the ready chains by loading its live-in values from the live-in register bank to the *IN*0 and *IN*1 registers. The scheduler also signals the fetch/decode unit in the lane to start issuing instructions. During chain execution, if an instruction produces a value that serves as a live-in to another chain, the value is written out to the one of the *OUT*0 or *OUT*1 registers. When the chain finishes executing, the values in the *OUT* registers are routed to the appropriate live-in register bank by the bus. Figure 8 shows a simple chained DFG that we use to demonstrate the architecture functions. Figure 8 also shows the execution sequence of chains belonging to this DFG, in their respective lanes. We assume a latency of one cycle for each operation. *C*0 executes first followed by *C*1 and *C*2.

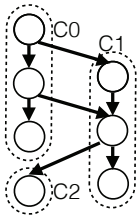

Instruction Fields

op	IN0/1	WR	FWD	L/R	OUT0/1
cvt	1	0	0	x	0
sub	0	1	1	1	1
sext	x	0	1	x	0

Scheduler Buffer

Chain	Lane	Live-in 0	Live-in 1	Child 0	Child 1
C0	Lane 0	-	-	C1	C1
C1	Lane 1	Reg 0	Reg 1	C2	-
C2	Lane 1	Reg 2	-	-	-

Schedule

Cycle	Lane 0	Lane 1
0	-	-
1	C0	-
2	C0	-
3	C0	-
4	-	-
5	-	C1
6	-	C1
7	-	C1
8	-	-
9	-	C2

Figure 8: Example DFG execution on *Chainsaw*.

Chain Scheduling and Wakeup

Figure 8 shows the scheduler table in the compiler for this DFG when mapped to a 2-lane ChainSaw. In this table, every row corresponds to a chain. The fields in a row respectively store the lane mapping, the register bank locations for live-ins, and the children chains. Since both the number of live-in values and live-out values are limited to two, it is sufficient to specify two children for each chain. For example, the row for *C*1 indicates i) the chain is mapped to execution lane 1, ii) the live-in values are stored at locations at register 0 and register 1 in the Live-in bank, and that *C*2 is its only child chain. The `Chain Ready` bits specify the chains mapped to the lane and whose dependencies are satisfied and ready for execution. When execution begins, all lanes are available. In the example, only *C*0 is ready to execute. Therefore, *C*0 is scheduled onto *Lane*0. When it finishes executing, its live-out values are present in register *OUT*0 and *OUT*1, both of which will be consumed by *C*1. The scheduler table entry for *C*1 gives the locations where these values must be routed to and the compiler inserts the appropriate move operations to terminate the chain. The bus routes these values, while *C*1 gets scheduled onto *Lane*1. Similarly, when *C*1 finishes, *C*2 is scheduled onto *Lane*1.

Instruction Issue

The fetch-decode unit in a lane sequentially fetches, decodes and issues instructions from the instruction buffer. The FU presents a simple 4-stage pipeline with the following stages: fetch, decode, execute, write register. Figure 8 shows the instruction buffer fields for chain *C*1. The *op* field gives the operation to be performed. *C*1 has three operations in the following sequence :*cvt*(convert), *sub*(subtraction), and, *sext*(sign extend). There are five 1-bit fields in each instruction: `IN0/1`, `WR`, `FWD`, `L/R`, `OUT0/1`. The `FWD` indicates whether one of the operands is available through bypassing i.e. the operand is the result of the previous chain operation. This field is clear for the first chain operation and set for subsequent chain operations. `IN0/1` indicates whether the instruction must read one live-in value from the IN0 register. For unary operations, this field is meaningful only if the operand is not available through value bypassing. For binary operations, this field is always meaningful because one of the inputs must be a live-in. Therefore this field is set in the first instruction as the only input is a live-in residing in IN0. This field is clear for the subtraction because, although it consumes a live-in, the value resides in IN1. This field is meaningless for the last instruction because it does not consume any live-ins. `L/R`, indicates the ordering among the operands. Ordering is meaningless for unary operations. However, for binary operations that are not commutative (e.g. subtraction), this field is necessary. Therefore, the subtraction defines this field whereas the other instructions do not. The `WR` determines whether the instruction produces a live-out. This flag is only set for the subtraction because it emits a live-out that is consumed by *C*2. The flag `OUT0/1` determines which of the OUT registers the value must be written to. It is set if the the destination is OUT0, and clear if the destination is OUT1.

6. Framework

We have built a LLVM–based toolchain for profiling, extracting chains and generating code for *Chainsaw*.

Profiling. The applications are profiled using `gprof` which identifies the critical functions and the function call hierarchy. Based on the `gprof` profile, we identify top-level functions that consume the largest amount of execution time. We then inline all functions called by this identified function in a bottom–up recursive manner. This LLVM–based infrastructure identifies paths [5] in the function. Enumerated paths are profiled using large representative inputs (eg. `ref` for SPEC benchmarks). Paths which include "unacceleratable" characteristics (such as external library calls, memory allocation) are pruned from the set.

We profile our workloads to understand how much "coverage" is provided by each path. Coverage of a path is calculated as the number of operations in the path times frequency of execution, represented as a fraction of the whole routine. Table 2 summarizes the coverage of the top five ranked paths in each workload. On average the coverage provided by the top five traces is 69% (median 88%). The five highest ranked paths by coverage are selected for chain extraction.

TABLE 2: ∑Coverage top five traces

$\sum_5$Cov.	Avg	Workloads
0-25	19%	sjeng, 401.bzip2
25-50	40%	blackscholes, bodytrack
50-75	64%	fluidanimate, freqmine, art
75-100	92%	h264ref, mcf, mcf, dwt53, namd, parser, soplex, gcc, gzip, equake, sphinx3, povray, hmmer, lbm

Chain Extraction. At the basic block granularity, there are no control dependences (basic blocks are terminated by branches). While chains can be derived from basic blocks, the blocks themselves are quite small in size (11 operations on avg, max 150 for namd). The *Chainsaw* architecture relies on the extraction of longer chains to reduce energy overheads by internalizing communication. To extract larger chains, we use an approach inspired by dynamic just-in-time compilers. All branches in the previously described outlined functions are converted to control flow assertions. The *Chainsaw* incorporates store buffers to export an atomic view of *Chainsaw* invocation. The average number of stores for all paths is 3, the maximum is 25. 97% of profiled paths had less than 16 stores.

The dataflow graph of the control free outlined function is constructed by examining each LLVM instruction and its operand. Chains are formed via the decomposition algorithms described in Section 4. The unmodified dataflow graph also serves as the basis of the CGRA timing simulation. We choose an optimistic CGRA schedule with no constraints.

Code Generation. The chain dataflow graph is derived from decomposing the original dataflow graph. The compiler adds the following information to the program binary: 1) markers to indicate regions that carry Chain information, 2) start addresses and lengths of chains in the region, 3) the dependencies among the chains belonging to the region, and 4) the stripped chain instructions (13 bits).

7. Evaluation

Simulation. We have developed a detailed cycle accurate simulator[1] that models the host core, the *Chainsaw* accelerator, and spatial fabrics of parameterizable size. The host OOO core pipeline is modelled using MacSim [35]. We assume that *Chainsaw* is an accelerator that communicates with the OOO core via the L1 cache. We model a CGRA, a spatial homogeneous fabric accelerator similar to [2], [3]. The memory hierarchy is modelled using Ruby [36]. We assume an aggressive non-blocking interface to memory. To accurately model the host-accelerator interaction via the memory system, we capture a window of memory accesses prior to the accelerator invocation and warm up the caches.The memory accesses for host execution and the accelerator are collected apriori using Intel Pin [37]. All memory operations from the host are collected in a trace. Memory operations at the IR level may not translate to an x86 instruction in the binary for the accelerated path.Thus IR level memory operations are marked in the binary during acceleration extraction in LLVM; the pin tool recognizes these accesses during tracing and dumps them to a separate accelerator trace. Each memory operation in the accelerator trace contains a unique identifier which maps it to a particular node in the dataflow graph. The *Chainsaw* and CGRA simulations use this trace to issue memory operations with addresses consistent with the host core.

We model all operations of the *Chainsaw* architecture as described in Section 5. To model the CGRA, we traverse the activity of the dataflow graph cycle-by-cycle, generating any requisite memory operations in a cycle and stalling the appropriate operations as necessary. To model the power consumption, we adopt an event-based power model similar to Aladdin [38]. Table 3 shows the characteristics of the architectures that we model.

TABLE 3: System parameters

Host Core	2 GHz, 4-way OOO, 96 entry ROB, 4 INT, 4 FPU, INT RF (64 entries), FP RF (64 entries) 32 entry load queue, 32 entry store queue
L1	64K 4-way D-Cache, 3 cycles
LLC	4M shared 16 way, 8 tile NUCA, ring, avg. 25 cycles. Directory MESI coherence.
Memory	200 cycles.
Accelerators	
CGRA8	8× 8 function units or
Chainsaw	Lane sizes:1,2,4,8,16 #instructions/lane:256,128,64,32,16.
Energy Parameters (Static and Dynamic)	
OOO	Mcpat [39]; ARM A9 2Ghz template.
CGRA8	CGRA Network (650 fJ/switch), Function units (510 fJ/INT,1500fJ/FP)
Chainsaw Lane	Instruction buffer (16 entries, 120 fJ/read, 220 fJ/write), Decode (100 fJ/ instruction)
Chainsaw Comm.	Pipeline forwarding (250 fJ), Live-in Registers (Read: 180fJ and Write: 250fJ), Bus (1100fJ/access)

1. The following six workloads crafty, freqmine, sar-back, sar-pfa, streamc.,swaptio. were not supported on our simulator.

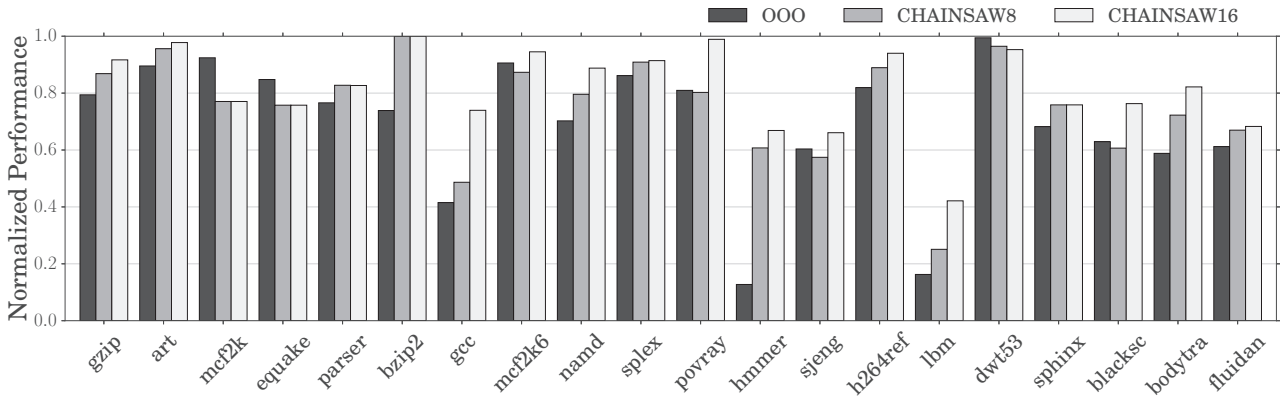

Figure 9: Performance of various architectures normalized to the IDEAL performance. We don't plot CGRA8 on this plot since in all applications the CGRA8 attains the performance of IDEAL. Higher is better.

Synthesis and Area Overhead . We designed the *Chainsaw* pipeline based on the RISC-V 4-stage IMAFD pipeline using our own custom instruction encoding. For synthesis, we used the Synopsys design compiler (Vision Z-2007.03-SP5) 45nm technology library. To tease out the impact of the main design tradeoffs we fix the design parameters of a single lane. The primary parameter that influences the complexity or overhead of a lane is the number of instruction buffer entries supported; our evaluation assumed 16 instructions per lane. Given that each instruction requires 13 bits (see Section 5) the entire instruction buffer in each lane requires 26 bytes and is single ported since the lanes are single issue. We picked this parameter to minimize the fetch overhead. The largest components in the lane design are the register banks which directly correlate with how many chains we would like to support and the number of chain dependencies which are the only communication that requires registers (see Figure 5). The sample configuration we synthesized and simulated supports 8 chains; given the maximum fan–in for many workloads is 1–2, we assumed a total of 2×8 registers per lane (i.e., 16 x 32 bit = 64 bytes). The register banks are dual ported to supply the chain registers in a single cycle. The scheduler, unlike OOO, consists of only one wakeup component; it does not require any tag matches since the compiler explicitly encodes the dependent children; each entry in the chain wakeup flag is 9 bits (1 bit for ready and two 4–bit live–in register ids). The chain wakeup matrix has as many entries as the number of chains per lane; (8×9 bits). Overall, the per lane overhead $\simeq$ 100 bytes (64 bytes for the 16 entry register bank, 26 bytes for the 8 entry instruction buffer, and 9 bytes for the chain wakeup flag). Overall, we found that the area for a 16 lane design ($\simeq$ 1.6 KB) is 0.21 mm^2 (including the functional units).

7.1. Performance Comparison

To understand the performance characteristics of the *Chainsaw* architecture, we compare *Chainsaw*8 and *Chainsaw*16 to a 4-wide OOO processor, an IDEAL-CGRA i.e. an unbounded CGRA that is only limited by the application[2] ILP. Figure 9 shows the performance of the OOO, *Chainsaw*8 and *Chainsaw*16 normalized with respect to the IDEAL-CGRA. Higher bars are better, i.e performance is closer to an IDEAL-CGRA.

For 10 of the 20 workloads (gzip, art, gcc, namd, soplex, hmmer, h264ref, lbm, bodytrack, and, fluidanimate), we find that performance of OOO $<$ *Chainsaw*8 $<$ *Chainsaw*16. In these benchmarks, the unchained DFG ILP (4–23 , see Table1) is greater than the width of the OOO core, therefore OOO is unable to exploit all the available ILP. The chained DFG ILP in the range 3–16, thus performance improves as the *Chainsaw* architecture is able to exploit more ILP. Of these there are three workloads (gcc, hmmer, and, lbm) with ILP in the range 6–16, for which *Chainsaw*16 performs significantly better than *Chainsaw*8 due to increased hardware resources.

For 6 workloads (mcf, equake, parser, bzip2, sphinx3, and, dwt53) the performance of the *Chainsaw*8 was the same as *Chainsaw*16. For all these workloads the chained DFG ILP is less than 8, thus *Chainsaw*16 is over-provisioned. In 3 of these workloads (mcf, equake and dwt53) the performance of the OOO is better than *Chainsaw* architectures. The chained ILP for each of these is less than the unchained ILP (see Figure 5) *as well as the average memory–level parallelism being lower than 3*. For the remaining workloads, the *Chainsaw* is able to exploit more MLP than OOO and improve performance.

For the remaining 4 workloads (mcf, povray, sjeng, blackscholes) we see an interesting pattern where the performance of the OOO is higher than *Chainsaw*8 but lower than *Chainsaw*16. In blackscholes, the OOO is marginally better than *Chainsaw*8 as the CPI is 8% less on average while the ILP is $\simeq$ 4. However, *Chainsaw*16 is significantly better than both the OOO and *Chainsaw*8 (upto 21%). *Chainsaw*16 is able to enqueue more long latency floating point operations in parallel than *Chainsaw*8. The number of idle cycles, cycle

2. We do not include the CGRA8x8 in this comparison as the fabric size restricts the number of operations. Of the 20 workloads we study, only 9 execute without reconfiguration ($<$ 64 ops, see Table1).

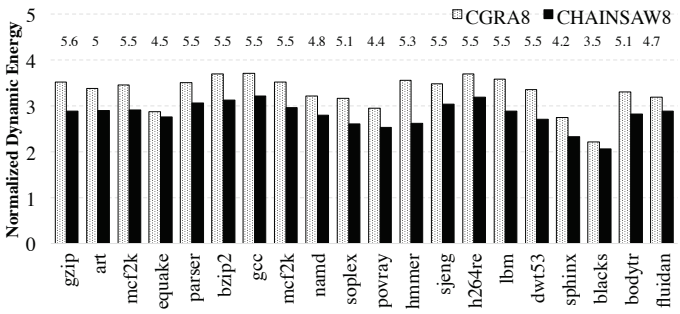

(a) Dynamic Energy. Data normalized to function unit energy i.e., > 1 indicates the overhead of the different architectures. The number on top of the bars for each workload indicates the OOO (includes the decode and backend costs; excludes TLBs and Caches). CGRA8 and CHAINSAW8 include all the components; CGRA overhead dominated by network energy.

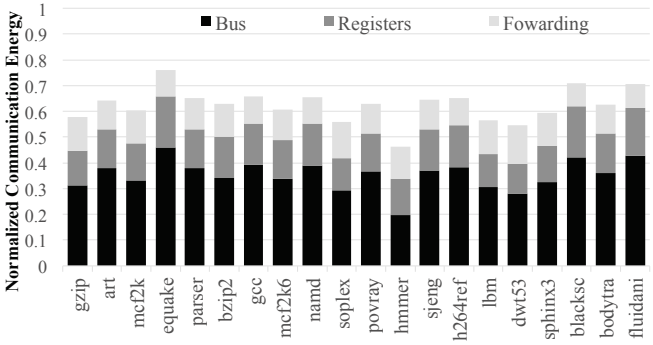

(b) Communication Energy Breakdown (*Chainsaw*8). Localized computation in CHAINSAW8 reduces communication costs significantly compared to dataflow architectures. The dominant energy component in both CHAINSAW8 and CGRA8 is the network transfers required between producer-consumer operations.

Figure 10: Dynamic Energy Comparison

count of ready chains blocked due to resource contention, is 3.4× for *Chainsaw*8 when compared to *Chainsaw*16. For the remaining 3 workloads, we see a common pattern of wide (>8) issue potential in the chain graph with long latency memory operations. The performance of the OOO with respect to *Chainsaw*8 is marginally better as the average ILP is only 3.4. The performance of *Chainsaw*16 is significantly better (average 9%) as it is able to overlap the long latency memory operations.

To summarize, in 8 of 20 workloads the performance of the *Chainsaw* architectures is within 90% of an unbounded dataflow. Across all workloads, the performance of *Chainsaw*16 is 81% and *Chainsaw*8 is 73% of an unbounded CGRA. *Chainsaw* architectures outperform an OOO core by 20.3% on average (17 out of 20 applications) with most significant improvements for gcc and hmmer.

7.2. Energy Comparison

Chainsaw and CGRA architectures represent two accelerator designs with different tradeoffs on various components of the total energy consumption. We first discuss dynamic power components, followed by static power. CGRA8 statically maps ops to the FUs, whereas *Chainsaw* incurs fetch-decode overhead per instruction. *Chainsaw* also incurs energy costs on chain activation and chain completion. On the other hand, *Chainsaw* attempts to minimize data movement, while CGRA8 moves data for every producer-consumer instruction pair. With regard to static power, CGRA8 is expected to have significant static power costs due to larger fabric size which leads to more idle cycles. *Chainsaw* improves utilization and limits static power.

Dynamic Energy Figure 10a shows the dynamic energy consumed by CGRA8 and *Chainsaw*8 normalized to functional unit energy. Across workloads the energy of the OOO (numbers above each bar) is $\simeq 5\times$ the functional unit energy. The least is found in blackscholes (50% floating point operations) and the most in gzip (only INT ops, no memory). The dynamic energy of the consumption of the CGRA8 is $\simeq 3.3\times$ the functional unit energy where the least is blackscholes. The most however is gcc where the link energy dominates due to the high connectivity of the dataflow graph. Similarly for the *Chainsaw*8, the average is $\simeq 2.8\times$. The net dynamic energy consumption is reduced via internalizing communication within chains.

Communication Costs Figure 10b shows the total energy expended by *Chainsaw* in communication, normalized to CGRA8 communication energy. Each benchmark is represented by a stacked bar, which shows the relative proportions of energy spent in the bus, pipeling forwarding, and register ($INs/OUTs$) communication by *Chainsaw*. The CGRA8 communication energy includes the fabric overhead and the latches at each PE. The reduction in communication cost is a motivation for the *Chainsaw* accelerator, because fetch-decode, which is the other component of dynamic power, is an essential component of von neumann style architectures. The chart shows that *Chainsaw* improves communication cost significantly, on average 38%. The variation in energy reduction is well illustrated by Figure 4a.

Although *Chainsaw* reduces bus events as far as possible, bus communication still consumes majority of the power. The dynamic energy cost of registers is related to the bus cost as each inter-chain dependence scheduled on a different lane triggers a bus access as well as a register access. Note that a bus access is 3.5× as expensive as pipeline forwarding. An inter-lane register write and then read is 44% more than forwarding. On average, forwarding events are 21% more frequent, with the highest occurrence in hmmer (2.2×). For 3 out of 20 workloads (equake, blackscholes, fluidanimate), the bus events are more frequent (average 30%) due to small chain formation (average size < 2 ops) coupled with greedy scheduling. The scheduling strategy is tuned for performance which seeks to schedule chains on free lanes to extract maximal ILP.

Overall, the dynamic communication energy is 38% lower for *Chainsaw*8 compared to CGRA8 due to conversion of link transfers to internal pipeline forwarding.

7.3. Static Power:

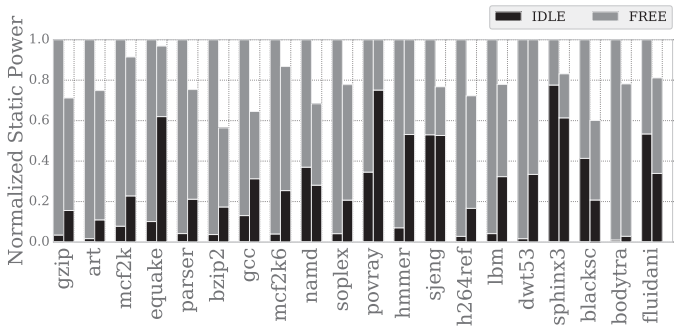

Figure 11: Static Power. CGRA8 and CHAINSAW8 normalized to CGRA8. IDLE : the static power expended while waiting for scheduled operations to be ready to run. FREE indicates the static power due to over-provisioning resources compared to the available ILP i.e., the PE or Lane does not have any instruction scheduled to execute.

Figure 11 shows the static power consumption normalized to the static power consumption of the CGRA8. The static power component is broken down into two components: the IDLE power and the FREE power. In lane or PE based execution such as *Chainsaw* and CGRA, a particular hardware resource might be inactive due to either the instruction assigned to the PE/lane has not been woken up yet since the producer instructions have not completed (IDLE), or the PE/Lane may have completed all the instructions assigned to it (FREE). The CGRA fabric for instruction-granularity accelerators [32] is scaled based on the number of operations to be accelerated while the *Chainsaw* is scaled based on the instruction parallelism available. Hence, in many cases the CGRA is excessively provisioned and is underutilized unless there is data parallelism to be exploited. This leads to an interesting case where the static power in the CGRA8 (64 units) is dominated by the FREE power; the FREE power may be curtailed by power-gating the PEs or the execution lanes. *Chainsaw*8 improves overall utilization and consumes much less FREE power but may introduce contention for the lanes or PEs by mapping multiple operations onto the same PE; this leads to an overall increase in IDLE power due to chain operations being stalled due to other unrelated chains occupying the lane. Note that both CGRA and *Chainsaw* will suffer from IDLE power since they statically map the operations to the resources.

*Chainsaw*8 reduces overall static energy by $\simeq$21%. From Figure 11, we see 11 of the 20 applications reduce energy by 20% to 40%. In equake, povray, hmmer, sjeng and lbm we see little to no reduction in overall static energy consumption. In all these applications a large fraction of the operations are long latency operations (FP or memory) thus increasing the IDLE'ness of the *Chainsaw*8. For 15 out of 20 workloads, there is more IDLE'ness in the *Chainsaw* architecture. In the remaining 5 workloads (namd, sjeng, blackscholes, bodytrack, fluidanimate), the IDLE'ness of the CGRA8 is more than the *Chainsaw* as even an unconstrained mapping leaves resources available due to the number of operations.

8. Conclusions

In this paper, we presented a new instruction abstraction, Chains, to exploit the producer-consumer locality between instructions. Chains present an effective strategy to localize communication between dependent instructions and save communication energy. Chains also enable the accelerator design to amortize the front-end costs. We have developed an end-to-end compiler prototype based on LLVM that extracts hot paths from applications, decomposes the dataflow graph into chains and prepares them for the *Chainsaw* architecture. *Chainsaw* is a lane-based architecture that leverages chains to achieve dynamic energy efficiency proportional to CGRA architectures, while minimizing idle and communication energy.

References

[1] T. Nowatzki and K. Sankaralingam, "Analyzing Behavior Specialized Acceleration." in *Proc. of the 21st ASPLOS*, 2016, pp. 697–711.

[2] H. Park, Y. Park, and S. Mahlke, "Polymorphic pipeline array: a flexible multicore accelerator with virtualized execution for mobile multimedia applications," in *PROC of the 42nd MICRO*, 2009.

[3] V. Govindaraju, C.-H. Ho, T. Nowatzki, J. Chhugani, N. Satish, K. Sankaralingam, and C. Kim, "Dyser: Unifying functionality and parallelism specialization for energy-efficient computing," *IEEE Micro*, vol. 32, no. 5, pp. 0038–51, 2012.

[4] C. Frericks, R. Cofell, and K. Sankaralingam, "Performance evaluation of a DySER FPGA prototype system spanning the compiler, microarchitecture, and hardware implementation," ... *Software (ISPASS)*, 2015.

[5] T. Ball and J. R. Larus, "Efficient Path Profiling," in *PROC of the 1996 MICRO*, 1996.

[6] S. Gupta, S. Feng, A. Ansari, S. Mahlke, and D. August, "Bundled execution of recurring traces for energy-efficient general purpose processing," in *PROC of the 44th MICRO*, 2011.

[7] C. González-Álvarez, J. B. Sartor, C. Alvarez, D. Jiménez-González, and L. Eeckhout, "Automatic design of domain-specific instructions for low-power processors," in *2015 IEEE 26th International Conference on Application-specific Systems, Architectures and Processors (ASAP)*. IEEE, 2015, pp. 1–8.

[8] R. Gonzalez, "Xtensa: a configurable and extensible processor," 2000.

[9] N. Clark, M. Kudlur, H. Park, S. Mahlke, and K. Flautner, "Application-Specific Processing on a General-Purpose Core via Transparent Instruction Set Customization," in *PROC of the 37th MICRO*, 2004.

[10] T. Nowatzki, V. Govindaraju, and K. Sankaralingam, "A Graph-Based Program Representation for Analyzing Hardware Specialization Approaches," *IEEE Computer Architecture Letters*, 2015.

[11] A. Lukefahr, S. Padmanabha, R. Das, F. M. Sleiman, R. G. Dreslinski, T. F. Wenisch, and S. A. Mahlke, "Composite Cores: Pushing Heterogeneity Into a Core." in *Proc. of the 45th MICRO*, 2012.

[12] S. Padmanabha, A. Lukefahr, R. Das, and S. A. Mahlke, "Trace based phase prediction for tightly-coupled heterogeneous cores." in *Proc. of the 46th MICRO*, 2013.

[13] R. Hameed, W. Qadeer, M. Wachs, O. Azizi, A. Solomatnikov, B. C. Lee, S. Richardson, C. Kozyrakis, and M. Horowitz, "Understanding sources of inefficiency in general-purpose chips," in *PROC of the 37th ISCA*, 2010.

[14] M. Hayenga, V. R. K. Naresh, and M. H. Lipasti, "Revolver: Processor architecture for power efficient loop execution." in *Proc. of the 20th HPCA*, 2014.

[15] T. Nowatzki, V. Gangadhar, and K. Sankaralingam, "Exploring the potential of heterogeneous von neumann/dataflow execution models," in *IEEE Computer Architecture Letters*, New York, New York, USA, Jun. 2015.

[16] G. Venkatesh, J. Sampson, N. Goulding, S. Garcia, V. Bryksin, J. Lugo-Martinez, S. Swanson, and M. B. Taylor, "Conservation cores: reducing the energy of mature computations," in *PROC of the 15th ASPLOS*, 2010.

[17] G. Venkatesh, J. Sampson, N. Goulding-Hotta, S. K. Venkata, M. B. Taylor, and S. Swanson, "Qscores: Trading dark silicon for scalable energy efficiency with quasi-specific cores," in *Proceedings of the 44th Annual IEEE/ACM International Symposium on Microarchitecture*. ACM, 2011, pp. 163–174.

[18] S. Hu, I. Kim, M. H. Lipasti, and J. E. Smith, "An approach for implementing efficient superscalar CISC processors," in *PROC of the 12th HPCA*, 2006.

[19] K. Sankaralingam, R. Nagarajan, R. McDonald, R. Desikan, S. Drolia, M. S. Govindan, P. Gratz, D. Gulati, H. Hanson, C. Kim, H. Liu, N. Ranganathan, S. Sethumadhavan, S. Sharif, P. Shivakumar, S. W. Keckler, and D. Burger, "Distributed Microarchitectural Protocols in the TRIPS Prototype Processor," in *PROC of the 39th MICRO*, 2006.

[20] E. Gibert, J. Sánchez, and A. González, "Flexible compiler-managed l0 buffers for clustered vliw processors," in *Proceedings of the 36th annual IEEE/ACM International Symposium on Microarchitecture*. IEEE Computer Society, 2003, p. 315.

[21] J. Balfour, "EFFICIENT EMBEDDED COMPUTING," 2011. [Online]. Available: http://cva.stanford.edu/publications/2010/jbalfour-thesis.pdf

[22] H.-S. Kim and J. E. Smith, "An instruction set and microarchitecture for instruction level distributed processing," in *PROC of the 29th ISCA*, 2002.

[23] D. Stasiak, R. Chaudhry, D. Cox, S. Posluszny, J. Warnock, S. Weitzel, D. Wendel, and M. Wang, "Cell processor low-power design methodology," in *Micro, ieee*, 2005.

[24] S. Larsen and S. Amarasinghe, "Exploiting superword level parallelism with multimedia instruction sets," in *PROC of the 2000 PLDI*, 2000.

[25] E. Ipek, M. Kirman, N. Kirman, and J. F. Martinez, "Core fusion: accommodating software diversity in chip multiprocessors," in *PROC of the 34th ISCA*, 2007.

[26] A. Ansari, S. Feng, S. Gupta, J. Torrellas, and S. A. Mahlke, "Illusionist: Transforming lightweight cores into aggressive cores on demand." in *Proc. of the 19th HPCA*, 2013.

[27] S. Padmanabha, A. Lukefahr, R. Das, and S. Mahlke, "Dynamos: dynamic schedule migration for heterogeneous cores," in *Proceedings of the 48th International Symposium on Microarchitecture*. ACM, 2015, pp. 322–333.

[28] M. Gebhart, S. W. Keckler, and W. J. Dally, "A compile-time managed multi-level register file hierarchy," in *PROC of the 44th MICRO*, 2011.

[29] P. Chen, L. Zhang, Y.-H. Han, and Y.-J. Chen, "A general-purpose many-accelerator architecture based on dataflow graph clustering of applications," *Journal of Computer Science and Technology*, vol. 29, no. 2, pp. 239–246, 2014.

[30] H. Park, K. Fan, S. A. Mahlke, T. Oh, H. Kim, and H.-s. Kim, "Edge-centric modulo scheduling for coarse-grained reconfigurable architectures," in *PROC of the 17th PACT*, 2008.

[31] S. Swanson, K. Michelson, A. Schwerin, and M. Oskin, "WaveScalar," in *PROC of the 36th MICRO*, 2003.

[32] V. Govindaraju, C.-H. Ho, and K. Sankaralingam, "Dynamically Specialized Datapaths for energy efficient computing," in *PROC of the 17th HPCA*, 2011.

[33] B. Dally, "Power, programmability, and granularity: The challenges of exascale computing," in *Parallel & Distributed Processing Symposium (IPDPS), 2011 IEEE International*. IEEE, 2011, pp. 878–878.

[34] D. R. Fulkerson, "Note on dilworths decomposition theorem for partially ordered sets," in *Proc. Amer. Math. Soc*, vol. 7. Citeseer, 1956, pp. 701–702.

[35] "Macsim : Simulator for heterogeneous architecture - https://code.google.com/p/macsim/." [Online]. Available: https://code.google.com/p/macsim/

[36] M. M. K. Martin, D. J. Sorin, B. M. Beckmann, M. R. Marty, M. Xu, A. R. Alameldeen, K. E. Moore, M. D. Hill, and D. A. Wood, "Multifacet's general execution-driven multiprocessor simulator (gems) toolset," *SIGARCH Comput. Archit. News*, vol. 33, no. 4, pp. 92–99, Nov. 2005. [Online]. Available: http://doi.acm.org/10.1145/1105734.1105747

[37] C.-K. Luk, R. Cohn, R. Muth, H. Patil, A. Klauser, G. Lowney, S. Wallace, V. J. Reddi, and K. Hazelwood, "Pin: building customized program analysis tools with dynamic instrumentation," in *ACM Sigplan Notices*, vol. 40, no. 6. ACM, 2005, pp. 190–200.

[38] Y. S. Shao, B. Reagen, G.-Y. Wei, and D. M. Brooks, "Aladdin: A pre-RTL, power-performance accelerator simulator enabling large design space exploration of customized architectures." in *Proc. of the 41st ISCA*, 2014, pp. 97–108.

[39] S. Li, J. H. Ahn, R. D. Strong, J. B. Brockman, D. M. Tullsen, and N. P. Jouppi, "McPAT: an integrated power, area, and timing modeling framework for multicore and manycore architectures," in *PROC of the 42nd MICRO*, 2009.